ISSN 1674-1056
http://cpb.iphy.ac.cn
http://iopscience.iop.org/cpb
中国物理 B
Chinese Physics
中国物理 Chinese Physics B

Equation of state for aluminum in warm dense matter regime

Kun Wang(王坤), Dong Zhang(张董), Zong-Qian Shi(史宗谦), Yuan-Jie Shi(石元杰), Tian-Hao Wang(王天浩), Yue Zhang(张阅)

Citation: Chin. Phys. B . 2019, 28(1): 016401. **doi:** 10.1088/1674-1056/28/1/016401
Journal homepage: http://cpb.iphy.ac.cn; http://iopscience.iop.org/cpb

What follows is a list of articles you may be interested in

Anomalous behavior and phase transformation of *α* -GaOOH nanocrystals under static compression

Zhao Zhang(张钊), Hang Cui(崔航), Da-Peng Yang(杨大鹏), Jian Zhang(张剑), Shun-Xi Tang(汤顺熙), Si Wu(吴思), Qi-Liang Cui(崔啟良)

Chin. Phys. B . 2017, 26(10): 106402. **doi:** 10.1088/1674-1056/26/10/106402

Correlation between electronic structure and energy band in Eu-doped $CuInTe_2$ semiconductor compound with chalcopyrite structure

Tai Wang(王泰), Yong-Quan Guo(郭永权), Shuai Li(李帅)

Chin. Phys. B . 2017, 26(10): 103101. **doi:** 10.1088/1674-1056/26/10/103101

Structure phase transformation and equation of state of cerium metal under pressures up to 51 GPa

Ce Ma(马策), Zuo-Yong Dou(窦作勇), Hong-Yang Zhu(祝洪洋), Guang-Yan Fu(付广艳), Xiao Tan(谈笑), Bin Bai(白彬), Peng-Cheng Zhang(张鹏程), Qi-Liang Cui(崔啟良)

Chin. Phys. B . 2016, 25(4): 046401. **doi:** 10.1088/1674-1056/25/4/046401

γ-and *α*-Ce phase diagram: First-principle calculation

Lin Zhang(张林), Ying-Hua Li(李英华), Xue-Mei Li(李雪梅), Zu-Gen Zhang(张祖根), Xiang-Ping Ye(叶想平), Ling-Cang Cai(蔡灵仓)

Chin. Phys. B . 2016, 25(3): 033102. **doi:** 10.1088/1674-1056/25/3/033102

Subsolidus phase relation in the Bi_2O_3–Fe_2O_3–La_2O_3 system

Hu Qi-Chang, Chen Ye-Qing, Lü Pei-Wen, Huang Feng, Wang Xian

Chin. Phys. B . 2014, 23(2): 026402. **doi:** 10.1088/1674-1056/23/2/026402

Equation of state for aluminum in warm dense matter regime*

Kun Wang(王坤)[1,2], Dong Zhang(张董)[1], Zong-Qian Shi(史宗谦)[3,†], Yuan-Jie Shi(石元杰)[3,4], Tian-Hao Wang(王天浩)[1], and Yue Zhang(张阅)[1]

[1] *State Key Laboratory of Reliability and Intelligence of Electrical Equipment, Hebei University of Technology, Tianjin* 300130, *China*
[2] *Key Laboratory of Electromagnetic Field and Electrical Apparatus Reliability of Hebei Province, Hebei University of Technology, Tianjin* 300130, *China*
[3] *State Key Laboratory of Electrical Insulation and Power Equipment, Xi'an Jiaotong University, Xi'an* 710049, *China*
[4] *Institute of Electronic Engineering, China Academy of Engineering Physics, Mianyang* 621999, *China*

(Received 27 July 2018; revised manuscript received 22 October 2018; published online 12 December 2018)

A semi-empirical equation of state model for aluminum in a warm dense matter regime is constructed. The equation of state, which is subdivided into a cold term, thermal contributions of ions and electrons, covers a broad range of phase diagram from solid state to plasma state. The cold term and thermal contribution of ions are from the Bushman–Lomonosov model, in which several undetermined parameters are fitted based on equation of state theories and specific experimental data. The Thomas–Fermi–Kirzhnits model is employed to estimate the thermal contribution of electrons. Some practical modifications are introduced to the Thomas–Fermi–Kirzhnits model to improve the prediction of the equation of state model. Theoretical calculation of thermodynamic parameters, including phase diagram, curves of isothermal compression at ambient temperature, melting, and Hugoniot, are analyzed and compared with relevant experimental data and other theoretical evaluations.

Keywords: equation of state, phase diagram, warm dense matter

PACS: 64.10.+h, 31.15.bu **DOI:** 10.1088/1674-1056/28/1/016401

1. Introduction

Warm dense matter, which demonstrates complicated physics due to strong interactions between particles,[1] is encountered in many engineering applications and fundamental research, such as cosmogony, inertial confined fusion, and *Z*-pinch. As an intermediate state between cold condensed matter and hot plasmas, warm dense matter is characterized by high densities as typical for condensed matter and temperatures of several eV.[2] The equations of state (EOS) in solid and ideal plasma states have already been established using perturbation theory and statistical physics, respectively. However, those theories are not feasible to calculate the properties of warm dense matter, in which partial ionization, strong correlations, and quantum effects are important, resulting in immense challenges to describe the behavior of warm dense matter accurately.[3]

EOS determines the fundamental thermodynamic properties of matter in hydrodynamic simulation. It is a crucial tool in interpreting the experimental results of warm dense matter.[4] The impressive progress in pulsed-power technology and diagnostics of high spatiotemporal resolution gives a great motivation in the investigation of warm dense matter.[5] The advanced experimental methods, such as dynamic compression using pulsed-power generator,[6] ablation with high-intensity laser,[7] generate extensive data of pressure to verify the EOS model. Since the warm dense matter occupies a broad range of phase diagram, a certain theory employed in EOS computations in specific density–temperature plane is difficult to cover the whole warm dense matter region. For instance, the chemical equilibrium model, in which several significant non-ideal effects are taken into consideration based on partially ionized plasma model, is commonly adopted to describe the thermodynamic properties for hot dense vapor and plasma.[8] Generally, different theories should be applied to the corresponding application range with special treatments in the transitional region to produce a global EOS table, such as the most commonly used SESAME database.[9] Much endeavor has been devoted to improve the prediction of EOS model in warm dense matter regime. Although the molecular dynamics and quantum Monte Carlo approaches have been employed in EOS computations,[10] applying reasonable models in different states to construct semi-empirical EOS model with corrections of experimental data is still a popular method. Bushman *et al.* developed a generalized semi-empirical EOS model for metals over a wide range of pressure and temperature.[11] Because it is easy to apply to different kinds of metallic materials with considerable accuracy, the multi-phase EOS model is further developed by Lomonosov.[12] The semi-empirical EOS model contains a number of adjusting parameters, which are fitted by relevant experimental data. The Frankfurt equation of state, which is applied to study the dynamics of vol-

*Project supported by the National Natural Science Foundation of China (Grant No. 51807050), the National Basic Research Program of China (Grant No. 2015CB251002) and the Program for the Top Young and Middle-aged Innovative Talents of Higher Learning Institutions of Hebei, China (Grant No. BJ2017038).

†Corresponding author. E-mail: zqshi@mail.xjtu.edu.cn

© 2019 Chinese Physical Society and IOP Publishing Ltd

umetrically heated matter passing through the liquid–vapor metastable states, is developed based on the quotidian equation of state (QEOS) scheme and, in principle, capable of generating EOS data for arbitrary materials as a function of density and temperature.[13] Although much work has been devoted to the EOS computations, the construction of EOS model of relatively high accuracy in warm dense matter regime remains a challenge.

In this paper, a semi-empirical EOS model for aluminum in warm dense matter regime is established. The EOS model consists of cold term, thermal contribution of ions, and thermal contribution of electrons. The key parameters in cold term and thermal contribution of ions are determined based on relevant experimental data. The thermal contribution of electrons is calculated by Thomas–Fermi–Kirzhnits model with some practical modifications. The theoretical results derived from the semi-empirical EOS model are compared with relevant experimental data and other theoretical calculations.

2. Equation of state model

The EOS model is subdivided into a cold term, thermal contributions of ions and electrons. The cold term is merely a function of density. The pressure P and internal energy E at a given density ρ and temperature T are expressed as follows:

$$P(\rho,T) = P_{\rm c}(\rho) + P_{\rm i}(\rho,T) + P_{\rm e}(\rho,T), \tag{1}$$

$$E(\rho,T) = E_{\rm c}(\rho) + E_{\rm i}(\rho,T) + E_{\rm e}(\rho,T). \tag{2}$$

The notations with subscripts of c, i, and e correspond to the parameters of cold term, thermal contribution of ions, and thermal contribution of electrons, respectively. Bushman[11] and Lomonosov[12] established a generalized semi-empirical EOS model for metals, accounting for solid, liquid, and gas states, as well as phase transitions of melting and vaporization. In the present work, the cold term and thermal contribution of ions are further divided into solid and liquid states. The free energy F is selected as a fundamental thermodynamic potential, because it is convenient to calculate the pressure and internal energy. The cold term for solid phase is expressed as[12]

$$F_{\rm c}^{\rm s}(\rho) = 3V_{0\rm c}\sum_{i=1,5}\frac{a_i}{i}\left(\sigma_{\rm c}^{i/3}-1\right), \tag{3}$$

where compression ratio $\sigma_{\rm c} = V_{0\rm c}/V$, specific volume $V = 1/\rho$, and $V_{0\rm c}$ is the specific volume at zero pressure. The variables a_i are determined by the best fitting between the pressure calculated by $F_{\rm c}^{\rm s}$ and the cold pressure of zero-temperature Thomas–Fermi–Kirzhnits model in the region of high compression ratio. The cold term for liquid phase in the compressed region ($\sigma_{\rm c} \geqslant 1$) is the same as Eq. (3), while the expression in the region of $\sigma_{\rm c} < 1$ is[12]

$$F_{\rm c}^{\rm l}(\rho) = V_{0\rm c}\left(A_{\rm c}\frac{\sigma_{\rm c}^m}{m} + B_{\rm c}\frac{\sigma_{\rm c}^n}{n} + C_{\rm c}\frac{\sigma_{\rm c}^l}{l}\right) + E_{\rm sub}, \tag{4}$$

where $E_{\rm sub}$ is the sublimation energy. $A_{\rm c}$, $B_{\rm c}$, $C_{\rm c}$, m, n, and l are also fitting parameters. The above parameters are estimated by the pressure, bulk compression modulus, and its pressure derivatives at the condition of $\sigma_{\rm c} = 1$. The free energy at $\sigma_{\rm c} = 1$ has a jump discontinuity, thus, a blending function is designed in the neighborhood of $\sigma_{\rm c} = 1$ for the cold term in liquid state to ensure that the free energy is continuously differentiable.[14]

The thermal contribution of ions in solid state, $F_{\rm i}^{\rm s}$, is calculated by high temperature approximations of Debye theory as[11]

$$F_{\rm i}^{\rm s}(\rho,T) = 3RT\ln\left(\frac{\theta^{\rm s}}{T}\right), \tag{5}$$

where R is the gas constant. $\theta^{\rm s}$ is an empirical relationship representing the characteristic temperature

$$\theta^{\rm s} = \theta_0^{\rm s}\exp\left(\frac{(\gamma_{0\rm s}-2/3)\left(B_{\rm s}^2+D_{\rm s}^2\right)}{B_{\rm s}}\arctan\left(\frac{xB_{\rm s}}{B_{\rm s}^2+D_{\rm s}(x+D_{\rm s})}\right)\right), \tag{6}$$

where $x = \ln(\sigma)$ and σ is the compression ratio. $\theta_0^{\rm s}$ is determined by the normalization condition for entropy $S = 0$ at normal conditions. The value of $\gamma_{0\rm s}$ is the tabulated value of Grüneisen parameter at ambient conditions.[12] $B_{\rm s}$ and $D_{\rm s}$ are found from the compression dependence of the Grüneisen parameter with the shockwave and isentropic compression data in solid state.[12]

The thermal contribution of ions in liquid state $F_{\rm i}^{\rm l} = F_{\rm i}^{\rm t} + F_{\rm i}^{\rm m}$. Here $F_{\rm i}^{\rm t}$ is the anharmonicity of ions at high temperatures[12] and ensures that the free energy is close to the asymptote of ideal gas in the high-temperature region

$$F_{\rm i}^{\rm t}(\rho,T) = \frac{3RT}{2}\left(1+\frac{\sigma T_{\rm a}}{(\sigma+\sigma_{\rm a})(T+T_{\rm a})}\right)\ln\left(\frac{\theta^{\rm l}}{T}\right), \tag{7}$$

where $\sigma_{\rm a}$ and $T_{\rm a}$ are the characteristic density and temperature in the transition of the heat capacity from the lattice value to that of an ideal atomic gas. $\theta^{\rm l}$ is also an empirical relationship representing the characteristic temperature in liquid phase.[12] $F_{\rm i}^{\rm m}$ models the melting effect, expressed as

$$F_{\rm i}^{\rm m}(\rho,T) = 3R\left[\frac{2\sigma_{\rm m}^2 T_{\rm m0}}{1+\sigma_{\rm m}^3}\left(C_{\rm m}+\frac{3A_{\rm m}}{5}\left(\sigma_{\rm m}^{5/3}-1\right)\right) + (B_{\rm m}-C_{\rm m})T\right], \tag{8}$$

where $\sigma_{\rm m} = \sigma/\sigma_{\rm m0}$, and $\sigma_{\rm m0}$ and $T_{\rm m0}$ are the compression ratio and melting temperature at standard pressure. $A_{\rm m}$, $B_{\rm m}$, and $C_{\rm m}$ are determined by the equilibrium conditions along the melting curve. The pressure and energy for the cold term and thermal contribution of ions can be calculated by the following thermodynamic functions:

$$P_{\rm c,i} = -\left(\frac{\partial F_{\rm c,i}}{\partial V}\right)_T, \tag{9}$$

$$E_{\mathrm{c,i}} = F_{\mathrm{c,i}} - T\left(\frac{\partial F_{\mathrm{c,i}}}{\partial T}\right)_V. \tag{10}$$

In the present work, the model for the thermal contribution of electrons is identical in solid, liquid, gas, and plasma states. The Thomas–Fermi–Kirzhnits model is applied to calculate the thermal contribution of electrons. The Thomas–Fermi model, which was initially developed to study the electron distribution of multi-electron atom, exhibits good performance for high Z (atomic number) elements. Since its advent, this model has been widely used in the EOS computations with advantages of clear physical picture and wide range of application.[15] The Thomas–Fermi model describes the behavior of electrons within an atom of Wigner–Seitz radius with the distribution of electron density $\rho(r)$ expressed as

$$\rho(r,p) = \frac{8\pi}{h^3}\frac{p^2}{\exp\left(\left(p^2/2m_{\mathrm{e}} - eU(r) - \mu\right)/k_{\mathrm{B}}T\right)+1}, \tag{11}$$

where p is the electron momentum, $U(r)$ is the electron potential, m_{e} is the electron mass, μ is the electron chemical potential, k_{B} is the Boltzmann constant, and h is the Planck constant. The electron potential is related to the electron density through Poisson's equation

$$\nabla^2 U(r) = 4\pi e\rho(r). \tag{12}$$

The second-order differential equation for the Thomas–Fermi model can be derived from the above equations with the parameter transformation of dimensionless potential $\varphi(x) = x(\mu + eU(r))/k_{\mathrm{B}}T$ and Fermi integral F_j. The Thomas–Fermi equation is expressed as

$$\varphi''(x) = axF_{1/2}\left(\frac{\varphi(x)}{x}\right), \tag{13}$$

where $x = r/r_0$, r_0 is the average radius of an atom, and $a = r_0(4\pi e(2m_{\mathrm{e}})^{3/4}(k_{\mathrm{B}}T)^{1/4}/h^{3/2})$. The boundary conditions for the Thomas–Fermi equation in center and outer boundary of an atom are $\varphi(0) = Ze^2/k_{\mathrm{B}}Tr_0$ and $\varphi(1) = \varphi'(1)$, respectively. The dimensionless potential can be achieved in an iterative algorithm with the boundary conditions applied. The thermodynamic parameters can be calculated by the dimensionless potential $\varphi(x)$,[16] for example, the pressure is expressed as

$$P_{\mathrm{TF}} = \frac{2}{9}\frac{a}{\varphi(0)}\frac{Zk_{\mathrm{B}}T}{V}F_{3/2}(\varphi(1)). \tag{14}$$

The Thomas–Fermi model, which yields a pressure of a few GPa under normal density at low temperatures, is only valid in the region of high compression ratio. In order to enlarge the application region of the Thomas–Fermi model, several corrections have been proposed to reduce the pressure to a reasonable level. Dirac introduced the electron exchange correction into the Thomas–Fermi model.[17] Later, the quantum effect, which had been proven to be an additional predominating term, was taken into consideration.[18] The Thomas–Fermi model with quantum and exchange corrections is denoted as the Thomas–Fermi–Kirzhnits model.[19] The perturbation equations of exchange and quantum corrections for the Thomas–Fermi model are respectively

$$\varphi_1''(x) - aF_{1/2}'\left(\frac{\varphi(x)}{x}\right)\varphi_1(x) = 6axF_{1/2}'^2\left(\frac{\varphi(x)}{x}\right), \tag{15}$$

$$\varphi_2''(x) - aF_{1/2}'\left(\frac{\varphi(x)}{x}\right)\varphi_2(x) = ax\left(F_{1/2}'^2\left(\frac{\varphi(x)}{x}\right) + F_{1/2}\left(\frac{\varphi(x)}{x}\right)F_{1/2}''\left(\frac{\varphi(x)}{x}\right)\right). \tag{16}$$

The exchange and quantum corrections on the thermodynamic parameters of the Thomas–Fermi model can be derived from Eqs. (15) and (16) with the boundary conditions $\varphi_i(0) = 0$ and $\varphi_i(1) = \varphi_i'(1)$ $(i = 1, 2)$. The pressure correction δP is calculated by the following equation:[20]

$$\delta P = \frac{Zk_{\mathrm{B}}T}{3V}\frac{ab}{\varphi(0)}\left(F_{1/2}(\varphi(1))\varphi_1(1) + F_{1/2}(\varphi(1))F_{1/2}'(\varphi(1)) + F_{1/2}(\varphi(1))\varphi_2(1) + 6\int_{-\infty}^{\varphi}F_{1/2}'^2(\xi)\,\mathrm{d}\xi\right), \tag{17}$$

where $b = (2m_{\mathrm{e}})^{1/2}e^2/3hk_{\mathrm{B}}^{1/2}T^{1/2}$.

The cold contributions of ions and electrons are included in the cold term of the EOS model. Therefore, the thermal contribution of electrons is estimated by the Thomas–Fermi–Kirzhnits model with subtraction of the zero-temperature part. The pressure generated by the Thomas–Fermi model is substantially reduced with the quantum and exchange corrections taken into consideration. It is found in the construction procedure of the present EOS model that the correction value for electrons is much larger than that predicted by the Thomas–Fermi model in a certain region, resulting in a large negative pressure for the thermal contribution of electrons. The negative pressure for electrons acts as a binding force in a material, however, this effect has already been included in the cold term. This factor may be responsible for the obvious deviation between the theoretical calculation based on the Thomas–Fermi–Kirzhnits model and experimental measurements. The Thomas–Fermi–Kirzhnits model is applicable in the region where the exchange and quantum corrections are no larger than the thermodynamic parameter of the Thomas–Fermi model.[21] This definition is adopted in the present EOS model. The thermal pressure of electrons P_{e} is calculated by the following practical modification in the present work:

$$P_{\mathrm{e}} = \begin{cases} P_{\mathrm{TF}} + \delta P, & P_{\mathrm{TF}} + \delta P \geqslant 0, \\ 0, & P_{\mathrm{TF}} + \delta P < 0. \end{cases} \tag{18}$$

The temperature–density boundary of $P_{\mathrm{TF}} + \delta P = 0$ for aluminum ($Z = 13$) is shown in Fig. 1. The thermal pressure for

electrons beyond the above applicable region of the Thomas–Fermi–Kirzhnits model is set to zero.

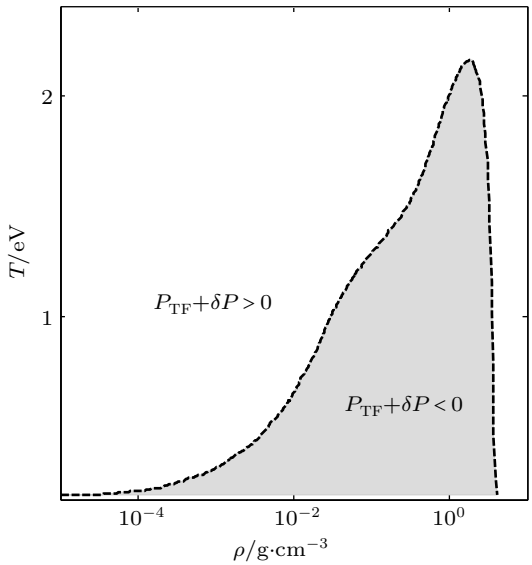


Fig. 1. The temperature–density boundary of $P_{\rm TF}+\delta P=0$ for aluminum calculated from the Thomas–Fermi–Kirzhnits model.

The operator expansion of the electron distribution used to evaluate the corrections in the Thomas–Fermi–Kirzhnits model appears to be asymptotic near the normal density at low temperature, yielding overcorrection to the pressure and internal energy.[19] This deficiency produces negative internal energy for the thermal contribution of electrons at low temperatures. The negative internal energy is encountered in some EOS models in certain density–temperature domain.[13,22] Generally, a normalization treatment is designed to generate non-negative minimum internal energy and pressure under normal conditions.[23] In the present work, the exchange and quantum corrections are not included in the electronic internal energy term to avoid negative total internal energy, making the EOS model approximately correct in this region.

3. Theoretical results and comparison with experimental data

Semi-empirical model is an important approach to calculate global EOS table for simulation of high energy density physics phenomena. The semi-empirical EOS model generates EOS data of different metal materials with relatively high accuracy and less calculation by adjusting several undetermined parameters. The fitting parameters in Table 1 for aluminum are determined based on the method described in the above section. In the construction process of the EOS model, the temperature, density, pressure, and internal energy are in units of kK, g/cm^3, GPa, and kJ/g, respectively.

Abundant pressure data at ambient temperature have been accumulated from a large number of isothermal compression experiments. Those data provide good benchmark for the cold term of EOS model in compressed solid state, because the thermal contribution constitutes a very small proportion of the results in compressed solid state at ambient temperature. The isothermal compression curve at ambient temperature calculated by this EOS model is presented in Fig. 2. The relevant experimental data[24–26] and theoretical evaluation[27] are also plotted for reference. The cold pressure is slightly lower than the pressure at room temperature. Generally, one can see from Fig. 2 that the isothermal compression curve agrees well with the experimental data, indicating that this EOS model generates reasonable predictions in the high-density region at low temperatures.

Table 1. Fitting parameters in the EOS model.

Variable	Value	Variable	Value	Variable	Value
V_{0c}	0.3614	B_c	40.96	D_s	0.36
a_1	326.35	C_c	−28.05	σ_a	0.923
a_2	−1035.4	m	8.0	T_a	30.0
a_3	851.51	n	4.99	σ_{m0}	0.923
a_4	−160.59	l	0.7	T_{m0}	0.933
a_5	11.17	θ_0^s	0.1	A_m	2.24
E_{sub}	12.098	γ_{0s}	2.19	B_m	−5.64
A_c	−12.91	B_s	0.6	C_m	0.21

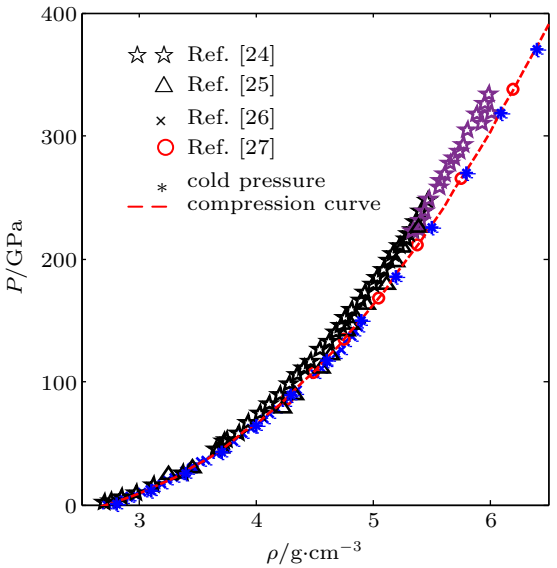


Fig. 2. The comparison of isothermal compression curve at ambient temperature with relevant experimental data and theoretical evaluation in compressed solid state.

The material behavior in condensed state at relatively high temperatures is one of the critical issues in EOS computations. The shock-compression experimental data is usually applied to verify the applicability of an EOS model in the region of high pressure and high temperature. If the shockwave propagates through a material, the thermodynamic parameter difference between the initial stage and behind the shockwave front is governed by the well-known Hugoniot relation[28]

$$E-E_0=\frac{1}{2}(P+P_0)\left(\frac{1}{\rho_0}-\frac{1}{\rho}\right), \tag{19}$$

where E_0, P_0, and ρ_0 are the internal energy, pressure, and density at the initial stage, respectively; and E, P, and ρ are the corresponding parameters after the interaction of shockwave front.

The relation between pressure and density (or compression ratio) in Hugoniot curve can be calculated from Eq. (19) combined with the EOS model. The comparison of Hugoniot curve and relevant shock-compression experimental data[29–33] and theoretical calculation[34,35] is shown in Fig. 3. The Hugoniot curve is calculated up to the density of 10 g/cm^3. It can be seen from Fig. 3 that the EOS predicts relatively accurate pressure along the Hugoniot curve with compression ratio ranging from 1 to 3.

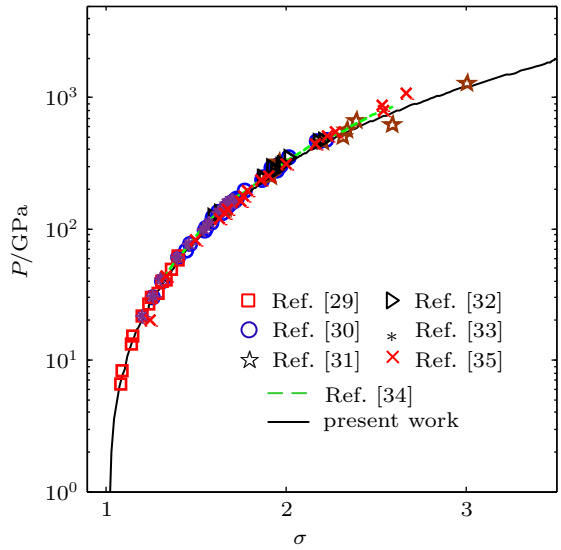


Fig. 3. Comparison of Hugoniot curve calculated by present EOS model with relevant shock-compression experimental data and theoretical evaluations.

The metal material may experience severe phase transition from solid state to plasma state under the intense loading dynamics in warm dense matter regime. For instance, the thin aluminum wire is exploded into liquid, gas, and plasma states with pulsed current flowing through the load. The phase diagram is particularly important for analyzing the phase transition of the metallic target. The theoretical results of the phase diagram for aluminum calculated by the EOS model are shown in Fig. 4. The melting curve in Fig. 4(a) presents the dependence of melting temperature on pressure. The melting density and temperature are determined by the equivalence of free energy for solid and liquid states. It can be seen from the comparison between melting curve and experimental data[36–38] in Fig. 4(a) that the calculated melting temperature in the region of low pressure is slightly lower than the experimental data, however, the relative error of the melting temperature is no more than 10%. The melting curve matches the experimental data very well in the relatively high-pressure region.

Figure 4(b) shows the pressure–density phase diagram of aluminum, including the isothermals for pressure (solid line), liquid–gas region (grey region with red dashed line for liquid–gas coexistence curve), melting region (grey region with boundary of red dotted line), critical point (red star), and relevant molecular dynamic simulations (circle and cross marks).[12,35] One can see from Fig. 4(b) that the isothermals for pressure are not monotonically increasing with density below the critical temperature, therefore, the saturated vapor pressure in liquid and gas phases at coexistence in the liquid–gas region can be calculated through Maxwell equal area rule. The branches for liquid and gas phases in coexistence curve connect at the critical point.

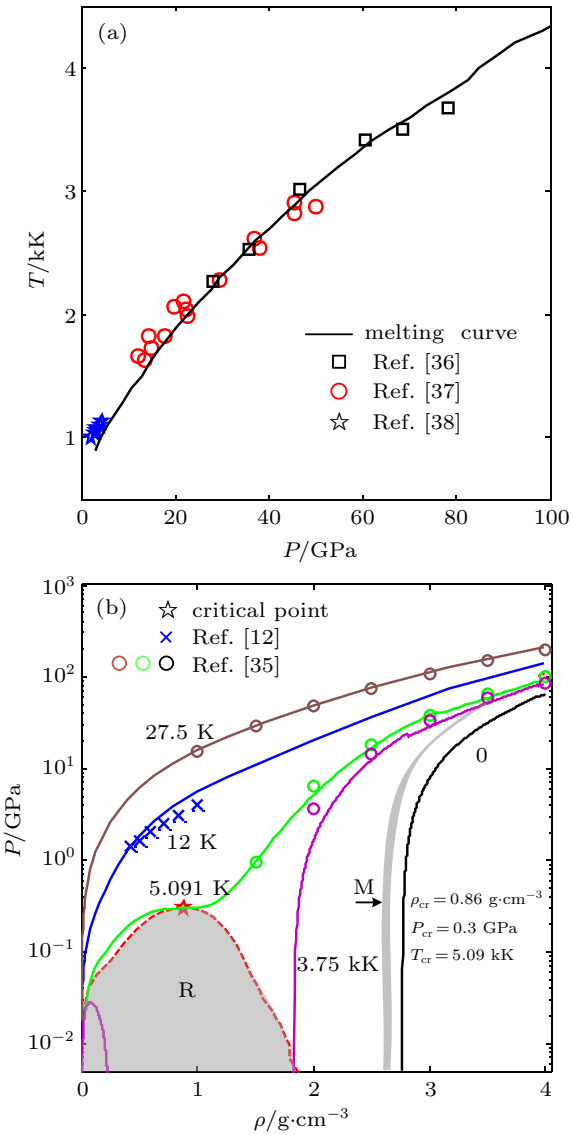


Fig. 4. The theoretical calculation of phase diagram and comparison with relevant experimental data and theoretical evaluations: (a) melting curve at high pressures; (b) pressure–density phase diagram (solid line: isothermals for pressure; R: liquid–gas region; M: melting region; circle/cross: molecular dynamic simulations; red star: critical point).

The parameters at the critical point are of great interest in many EOS computations. The critical density, temperature, and pressure are 0.86 g/cm^3, 5.091 kK, and 0.3 GPa, respectively. A collection of estimated values of critical parameters

for aluminum[23,39,40] is presented in Table 2. The theoretical estimations for the critical parameters of aluminum from various EOS models exhibit relatively large variations. The critical temperature reported in many literatures ranges from 4.744 kK to 12.1 kK. The critical compressibility factor Z_c is usually used to compare the deviation of those critical parameters of different EOS models. The critical compressibility factor $Z_c = 0.222$ in the present work is close to the results derived by the soft-sphere model ($Z_c = 0.243$) and grand-canonical transition matrix Monte Carlo method ($Z_c = 0.249$).[41]

Table 2. The collection of critical parameters for aluminum.

T_{cr}	P_{cr}	ρ_{cr}	Z_c	Ref.
7.222	0.571	0.806	0.318	[11]
7.917	0.467	0.660	0.290	[23]
4.744–8.550	0.172–0.586	0.400–0.690		[39]
5.726	0.182	0.424	0.243	[40]
8.742	0.509	0.785	0.249	[41]
5.091	0.300	0.860	0.222	this work

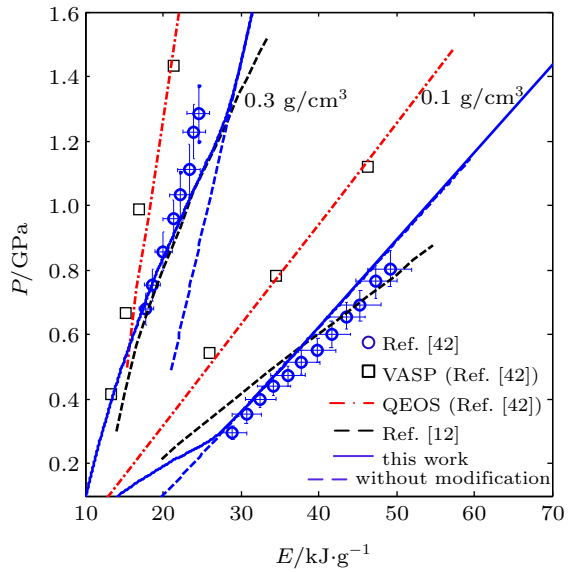


Fig. 5. The pressure as a function of internal energy at densities of 0.1 g/cm^3 and 0.3 g/cm^3 derived by the present EOS model and comparison with isochore measurements and other theoretical models.

The pressure and internal energy variation of aluminum at densities of 0.1 g/cm^3 and 0.3 g/cm^3 were measured using a homogeneous and thermally equilibrated plasma produced inside a closed vessel in the energy range 20–50 kJ/g by Renaudin[1] and the isochore measurements were frequently used to verify the newly-established EOS models in warm dense matter regime. The pressure as a function of internal energy at densities of 0.1 g/cm^3 and 0.3 g/cm^3 derived from the present EOS model and comparison with experimental data are shown in Fig. 5. The theoretical results from QEOS, VASP calculated in Ref. [1] and results calculated by Lomonosov[12] are also plotted in Fig. 5 for reference. One can see from Fig. 5 that the results from the present EOS model fit the experimental measurements relatively better among the theoretical models. The blue dashed line presents the results without practical modification of Eq. (18) to the pressure of the Thomas–Fermi–Kirzhnits model. The EOS model without pressure modification accords with experimental data at the density of 0.1 g/cm^3, while generates noticeably lower pressure than experimental measurements at the density of 0.3 g/cm^3. The value and variation trend in internal energy–pressure isochore curve of 0.3 g/cm^3 is greatly improved with practical modification made to the Thomas–Fermi–Kirzhnits model.

4. Conclusion

A semi-empirical EOS model for aluminum in warm dense matter regime is constructed. The EOS model consists of three terms, i.e., the cold term, thermal contributions of ions and electrons. The Bush–Lomonosov model is used to estimate the cold term and thermal contribution of ions, while the thermal contribution of electrons is calculated based on the Thomas–Fermi–Kirzhnits model. The practical modifications are introduced to the Thomas–Fermi–Kirzhnits model to improve the prediction. The definition of applicable region of the Thomas–Fermi–Kirzhnits model from the condition of smallness of the corrections in comparison with thermodynamic parameter themselves is adopted to reshape the configuration of pressure. The minimum pressure for the thermal contribution of electrons is set to be zero artificially in the region where pressure depression from exchange and quantum corrections is larger than that derived from the Thomas–Fermi model. The critical parameters predicted by the EOS model are 0.86 g/cm^3, 0.3 GPa, and 5.091 kK, respectively, giving a critical compressibility factor of 0.222. The isothermal compression curve, melting curve, and Hugoniot curve, as well as phase diagram are analyzed and compared with relevant experimental data and theoretical evaluations. The dependence of pressure on internal energy is verified by the isochore measurements in the warm dense matter regime. Generally speaking, the predictions of the EOS model are in relatively good agreement with the experimental data. This EOS model will be applied in the numerical investigation on the behavior of metallic target under the intense action of pulsed current in the future work, such as exploding wires and wire-array Z-pinch.

References

[1] Renaudin P, Blancard C, Clérouin J, Faussurier G, Noiret P and Recoules V 2003 *Phys. Rev. Lett.* **91** 075002

[2] Lorenzen W, Becker A and Redmer R 2014 *Frontiers and Challenges in Warm Dense Matter, Lecture Notes in Computational Science and Engineering* (Graziani F, Desjarlais M P, Redmer R and Trickey S B, Ed.) (Cham: Springer) Vol. **96**, pp. 203–204

[3] Chen Q F, Gu Y J, Zheng J, Li J T, Li Z G, Long Q W, Fu Z J and Li C J 2017 *Chin. Sci. Bull.* **62** 812 (in Chinese)

[4] Lomonosov I V and Gryaznov V K 2016 *Contrib. Plasma Phys.* **56** 302

[5] Desilva A W and Vunni G B 2011 *Phys. Rev. E* **83** 037402

[6] Knudson M D, Desjarlais M P, Becker A, Lemke R W, Cochrane K R, Savage M E, Bliss D E, Mattsson T R and Redmer R 2015 *Science* **348** 1455

[7] Mostovych A N, Chan Y, Lehecha T, Phillips L, Schmitt A and Sethian J D 2000 *Phys. Rev. Lett.* **85** 3870

[8] Zaghloul M R 2018 *High Energy Density Phys.* **26** 8

[9] Kashiwa B A 2010 *The MGGB equation-of-state for multifield applications: a numerical recipe for analytic expression of sesame EOS data* (Los Alamos National Laboratory Report: LA-14421)

[10] Li Z G, Cheng Y, Chen Q F, Chen X R 2016 *Phys. Plasmas* **23** 052701

[11] Bushman A V, Kanel G I, Ni A L and Fortov V E 1993 *Intense Dynamic Loading Condens. Matter* (Bosa Roca: Taylor & Francis) pp. 116–141

[12] Lomonosov I V 2007 *Laser Part. Beams* **25** 567

[13] Faika S, Tauschwitz A, Iosilevskiy I, Maruhn J A 2012 *High Energy Density Phys.* **8** 349

[14] Wang K, Shi Z Q, Shi Y J, Wu J, Jia S L and Qiu A C 2015 *Acta Phys. Sin.* **64** 156401 (in Chinese)

[15] Shemyakin O P, Levashov P R and Khishchenko K V 2012 *Contrib. Plasma Phys.* **52** 37

[16] Wang K, Shi Z Q, Shi Y J, Bai J, Wu J and Jia S L 2015 *Phys. Plasmas* **22** 062709

[17] Dirac P A M 1930 *Proc. Cambridge Philos. Soc.* **26** 376

[18] Kirzhnits D A 1957 *Sov. Phys. JETP* **5** 64

[19] McCarthy S L 1965 *The Kirzhnits Corrections to the Thomas–Fermi Equation of State* (Lawrence Livermore Laboratory Report: UCRL-14364)

[20] Yu G R 1987 *Journal of Xinyang Nornal University (Natural Science Edition)* **1** 1 (in Chinese)

[21] Dyachkov S and Levashov P 2014 *Phys. Plasmas* **21** 052702

[22] Cochrane K, Desjarlais M, Haill T, Lawrence J, Knudson M and Dunham G 2006 *Aluminum Equation of State Validation and Verification for the ALEGRA HEDP Simulation Code* (Sandia National Laborary Report: SAND2006-1739)

[23] Gordeev G D, Gudarenko L F, Zhernokletov M V, Kudel'Kin V G and Mochalov M A 2008 *Combustion Explosion & Shock Waves* **44** 177

[24] Akahama Y, Nishimura M, Kinoshita K, Kawamura H, Ohishi Y 2006 *Phys. Rev. Lett.* **96** 045505

[25] Greene R G, Luo H and Ruoff A L 1994 *Phys. Rev. Lett.* **73** 2075

[26] Dewaele A, Loubeyre P, Mezouar M 2004 *Phys. Rev. B* **70** 094112

[27] Nellis W, Moriarty J, Mitchell A, Ross M, Dandrea R, Ashcroft N, Holmes N and Gathers G 1988 *Phys. Rev. Lett.* **60** 1414

[28] Eliezer S, Ghatak A K, Hora H and Ghatak A 2002 *Fundamentals Equations State* (Singapore: World Scientific) p. 165

[29] Marsh S P 1980 *LASL Shock Hugoniot Data* (London: Cambridge University Press) p. 23

[30] Celliers P M, Collins G W, Hicks D G and Eggert J H 2005 *J. Appl. Phys.* **98** 113529

[31] Trunin R F, Panov M V and Medvedev A B 1995 *JETP Lett.* **62** 591

[32] Knudson M D, Lemke R W, Hayes D B, Hall C A, Deeney C and Asay J R 2003 *J. Appl. Phys.* **94** 4420

[33] Mitchell A C and Nellis W J 1981 *J. Appl. Phys.* **52** 3363

[34] Fu Z J, Quan W L, Zhang W, Li Z G, Zheng J, Gu Y J and Chen Q F 2017 *Phys. Plasmas* **24** 013303

[35] Minakov D A, Levashov P R, Khishchenko K V and Fortov V E 2014 *J. Appl. Phys.* **115** 223512

[36] Boehler R and Ross M 1997 *Earth & Planet. Sci. Lett.* **153** 223

[37] Hänström A and Lazor P 2000 *J. Alloys & Compd.* **305** 209

[38] Jayaraman A, Klement J W and Kennedy G C 1963 *Phys. Rev.* **130** 2277

[39] Ohse R W and Tippelskirch H V 1977 *High Temperatures-High Pressures* **9** 367

[40] Young D A 1977 *Soft-sphere model for liquid metals* (Lawrence Livermore Laboratory Report: UCRL-52352)

[41] Singh J K, Adhikari J and Sang K K 2006 *Fluid Phase Equilibria* **248** 1